

# Polymorphs of a diarylethene that exhibits strong emission and direct visualization of polymorphic phase transition process by fluorescence color change

メタデータ	言語: English 出版者: Elsevier 公開日: 2019-04-26 キーワード (Ja): キーワード (En): Diarylethene, Crystal, Strong emission, Polymorphs, Phase transition, Visualization 作成者: 北川, 大地, 中濱, 龍源, 武藤, 克也, 小林, 洋一, 阿部, 二郎, 五月女, 光, 伊都, 将司, 宮坂, 博, 小畠, 誠也 メールアドレス: 所属: Osaka City University, Osaka City University, Aoyama Gakuin University, Aoyama Gakuin University, Aoyama Gakuin University, Osaka University, Osaka University, Osaka University, Osaka University, Osaka City University
URL	<a href="https://ocu-omu.repo.nii.ac.jp/records/2019812">https://ocu-omu.repo.nii.ac.jp/records/2019812</a>

# Polymorphs of a diarylethene that exhibits strong emission and direct visualization of polymorphic phase transition process by fluorescence color change

Daichi Kitagawa, Tatsumoto Nakahama, Katsuya Mutoh, Yoichi Kobayashi, Jiro Abe, Hikaru Sotome, Syoji Ito, Hiroshi Miyasaka, Seiya Kobatake

<b>Citation</b>	Dyes and Pigments, 139; 233-238
<b>Issue Date</b>	2017-04
<b>Type</b>	Journal Article
<b>Textversion</b>	author
<b>Supplementary data</b>	Supplementary data is available at <a href="https://doi.org/10.1016/j.dyepig.2016.12.006">https://doi.org/10.1016/j.dyepig.2016.12.006</a> .
<b>Rights</b>	©2017. This manuscript version is made available under the CC-BY-NC-ND 4.0 License. <a href="http://creativecommons.org/licenses/by-nc-nd/4.0/">http://creativecommons.org/licenses/by-nc-nd/4.0/</a> . The article has been published in final form at <a href="https://doi.org/10.1016/j.dyepig.2016.12.006">https://doi.org/10.1016/j.dyepig.2016.12.006</a>
<b>DOI</b>	10.1016/j.dyepig.2016.12.006

Self-Archiving by Author(s)  
Placed on: Osaka City University

KITAGAWA, D., NAKAHAMA, T., MUTOH, K., KOBAYASHI, Y., ABE, J., SOTOME, H., ITO, S., MIYASAKA, H., & KOBATAKE, S. (2017). Polymorphs of a diarylethene that exhibits strong emission and direct visualization of polymorphic phase transition process by fluorescence color change. *Dyes and Pigments*. 139, 233-238.

# Polymorphs of a diarylethene that exhibits strong emission and direct visualization of polymorphic phase transition process by fluorescence color change

*Daichi Kitagawa,<sup>a</sup> Tatsumoto Nakahama,<sup>a</sup> Katsuya Mutoh,<sup>b</sup> Yoichi Kobayashi,<sup>b</sup> Jiro Abe,<sup>b</sup> Hikaru Sotome,<sup>c</sup> Syoji Ito,<sup>c</sup> Hiroshi Miyasaka,<sup>c</sup> Seiya Kobatake<sup>\*,a</sup>*

<sup>a</sup>Department of Applied Chemistry, Graduate School of Engineering, Osaka City University, 3-3-138 Sugimoto, Sumiyoshi-ku, Osaka 558-8585, Japan.

<sup>b</sup>Department of Chemistry, School of Science and Engineering, Aoyama Gakuin University, 5-10-1 Fuchinobe, Chuo-ku, Sagami-hara, Kanagawa 252-5258, Japan

<sup>c</sup>Division of Frontier Materials Science and Center for Promotion of Advanced Interdisciplinary Research, Graduate School of Engineering Science, Osaka University, Toyonaka, Osaka 560-8531, Japan

## **Corresponding Author**

\* [kobatake@a-chem.eng.osaka-cu.ac.jp](mailto:kobatake@a-chem.eng.osaka-cu.ac.jp).

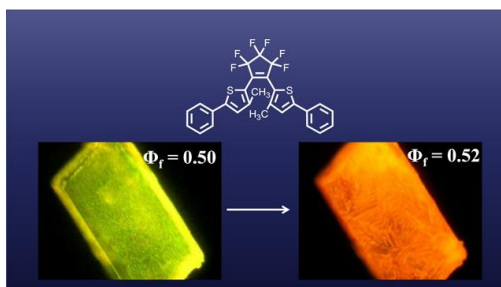
## ABSTRACT

Luminescent solid-state materials with high fluorescence quantum yield have attracted much attention in application to organic optoelectronics. In the course of study of photochromic diarylethene crystals, we found that two polymorphic forms of a diarylethene are obtained by recrystallization from acetone and *n*-hexane solutions. Surprisingly, both polymorphic crystals exhibited strong emission whose fluorescence quantum yield ( $> 0.5$ ) is much higher than that in *n*-hexane solution (0.017). Furthermore, the thermodynamic solid-state polymorphic phase transition was found and the process was directly visualized by a fluorescence color change.

## KEYWORDS

Diarylethene, Crystal, Strong Emission, Polymorphs, Phase Transition, Visualization

## Graphical Abstract

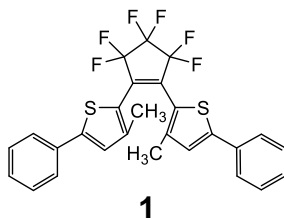


## 1. Introduction

Luminescent solid-state materials have attracted much attention in various applications such as organic light-emitting diodes [1], optical waveguides [2], optically pumped lasers [3], and sensory materials [4]. However, the luminescent intensity is often decreased in the solid state as compared with in the solution due to the aggregation-caused quenching. To overcome this point, many researchers have reported several types of organic molecules that exhibit strong fluorescence even in the solid state [5-7]. Especially, molecules that exhibit aggregation-induced enhanced emission (AIEE) have been widely investigated [7-9]. They exhibit weak or no emission in solution, but exhibit strong emission in the solid state. To investigate a new type of molecules having AIEE character is one of the important challenges in the research field of the luminescent solid-state materials.

On the other hand, visualization of various processes such as nucleation, crystallization, amorphousization, amorphous-to-crystal transformation, hardening and freezing by utilizing fluorescence color change has been also examined [10-14]. The fluorescence color depends on the molecular environment and aggregation state. Tao *et al.* reported on the crystallization process of fluorenyl-containing tetrasubstituted ethylene microparticles accompanying fluorescence color change [10]. They have succeeded in the direct observation of the process of the transformation from the metastable amorphous state to the crystalline state. Recently, Ito *et al.* have also reported the direct visualization of the two-step nucleation model for organic molecular crystallization by fluorescence color change [11]. When the crystal of a dibenzoyl boron complex was crystallized out, the transitional emission from the amorphous cluster state prior to crystallization can be detected. This result supports the two-step nucleation model, in which the crystallization process includes the formation of a liquid-like cluster or an amorphous cluster. The revelation of the mechanism in such processes brings about not only new fundamental perspectives but also strategies for design of novel functional organic solid materials.

Photochromic diarylethenes have attracted much attention for application to optical memory media, switching devices, and display materials. Although there are many studies on the photochromic reaction in the crystalline phase and its applications, there is little research that focuses on the fluorescence property of diarylethenes in the solid state. In the course of study on photochromic diarylethene crystals [15-20], we have found polymorphism of a diarylethene, 1,2-bis(3-methyl-5-phenyl-2-thienyl)perfluorocyclopentene (**1**) (Scheme 1). In *n*-hexane solution, diarylethene **1** undergoes reversible photochromic reactions with photocyclization quantum yield of 0.17 and photocycloreversion quantum yield of 0.48 and emits fluorescence in the open-ring isomer with fluorescence quantum yield of 0.017 [21]. On the other hand, the diarylethene does not undergo photochromism in the crystalline state and the polymorphic crystals exhibit strong emission with different fluorescence colors. In this work, we have first observed that the diarylethene exhibits AIEE in the crystalline state and the phase transition between polymorphs accompanying fluorescence color change.



**Scheme 1.** Molecular structure of diarylethene **1**

## 2. Experimental

### 2.1. General

Polymorphic crystals were observed using a Keyence VHX-500 digital microscope. UV irradiation was carried out using a Keyence UV-LED UV-400 (365-nm light). Diffuse reflectance spectra were measured using a JASCO V-560 absorption spectrophotometer equipped with a JASCO ISV-469 integrating sphere. Fluorescence spectra were measured with a

JASCO FP-8300 fluorescence spectrometer. Fluorescence quantum yields were also determined with a JASCO FP-8300 fluorescence spectrometer equipped with a JASCO ILF-835 integrate sphere. Polymorphic phase transition of crystals was observed using a Nikon ECLIPSE E600POL polarizing optical microscope, equipped with a Mettler-Toledo FP82HT hot stage and FP90 central processor. Differential scanning calorimetry (DSC) was run using a HITACHI DSC-7000X. Thermogravimetric analysis (TGA) was run using a SII TG/DTA 6200. Powder X-ray diffraction profiles were recorded on a Rigaku RINT-2100 diffractometer employing  $\text{CuK}\alpha$  radiation ( $\lambda = 1.54184 \text{ \AA}$ ). Single crystal X-ray crystallographic analysis was carried out using a Rigaku AFC/Mercury CCD diffractometer with  $\text{MoK}\alpha$  radiation ( $\lambda = 0.71073 \text{ \AA}$ ) monochromated by graphite. The crystal structures were solved by a direct method using SIR92 and refined by the full-matrix least-squares method on  $F^2$  with anisotropic displacement parameters for non-hydrogen atoms using SHELXL-97.

## 2.2. Fluorescence lifetime measurement

Time profiles of the fluorescence of polymorphic crystals were measured using a time-correlated single-photon-counting (TCSPC) system with a Ti:sapphire laser as a pulsed light source (Spectra-Physics, Tsunami, 80 MHz, ca. 100-fs fwhm). An experimental setup of the TCSPC system was described elsewhere [22]. The fundamental output at 870 nm of the Ti:sapphire laser was converted into the 540 nm pulse by using a photonic crystal fiber (NKT Photonics, FemtoWHITE800). The excitation beam was introduced into the samples after removing the remaining near-infrared light by a bandpass filter. The repetition rate was reduced to 8 MHz by an electro-optic modulator (Conoptics, Model 350). The excitation power at the sample position was typically  $4.4 \mu\text{W}$  at 8 MHz. Fluorescence signal was detected at the magic angle configuration with a film polarizer and Babinet-Soleil compensator. A photomultiplier-tube (Hamamatsu Photonics, R3809U-50) equipped with a pre-amplifier (Hamamatsu Photonics, C5594) and a TCSPC module (PicoQuant, PicoHarp 300) were used. A monochromator

(Princeton Instruments, Acton SP-2150) was placed in front of the photomultiplier-tube. The crystalline samples were retained using a pair of glass plates. The typical response time of the system was 100 ps (fwhm), which was determined by detecting scattered photons from a scratched glass plate.

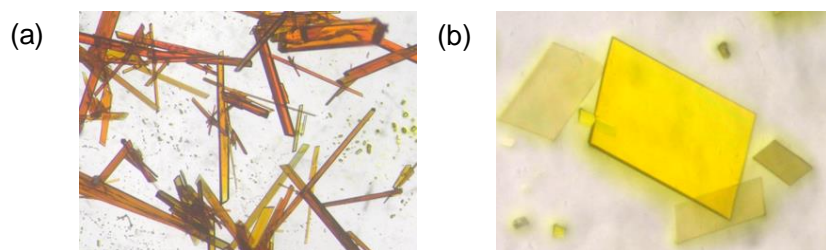
### 2.3. Materials

Diarylethene **1** was synthesized by the method described in the literature [21].

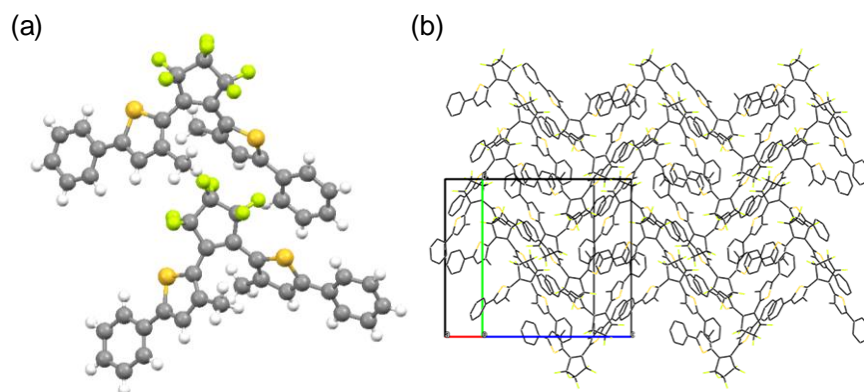
## 3. Results and Discussion

Fig. 1 shows the photographs of single crystals of diarylethene **1** observed under normal view. When diarylethene **1** was recrystallized from acetone, the orange needle crystal, called  $\alpha$ -crystal, can be obtained [21]. On the other hand, the yellow platelet crystal, called  $\beta$ -crystal, can be obtained when diarylethene **1** was recrystallized from *n*-hexane. To clarify the polymorphic forms of these crystals, single crystal X-ray crystallographic analysis was performed. Molecular packing diagrams of  $\alpha$ - and  $\beta$ -crystals are shown in Figs. 2 and 3, respectively. The crystallographic data are summarized in Table 1. The crystal systems and space groups of  $\alpha$ - and  $\beta$ -crystals were monoclinic  $P2_1/c$  and triclinic  $P\bar{1}$ , respectively. The  $\alpha$ -crystal consists of eight diarylethene molecules in the unit cell and two diarylethene molecules in the asymmetric unit, while the  $\beta$ -crystal has two diarylethene molecules and one hexane molecule in the unit cell and one diarylethene molecule and a half of hexane molecule in the asymmetric unit. These results indicate that  $\alpha$ - and  $\beta$ -crystals are evidently polymorphic forms.





**Fig. 1.** Optical microscopic photographs of single crystals of diarylethene **1**: (a)  $\alpha$ -crystal and (b)  $\beta$ -crystal.



**Fig. 2.** Crystal structure of  $\alpha$ -crystal (a) in the asymmetric unit and (b) molecular packing viewed from  $(100)$ . The perfluorocyclopentene rings were disordered. Only a conformer was illustrated for clarity.

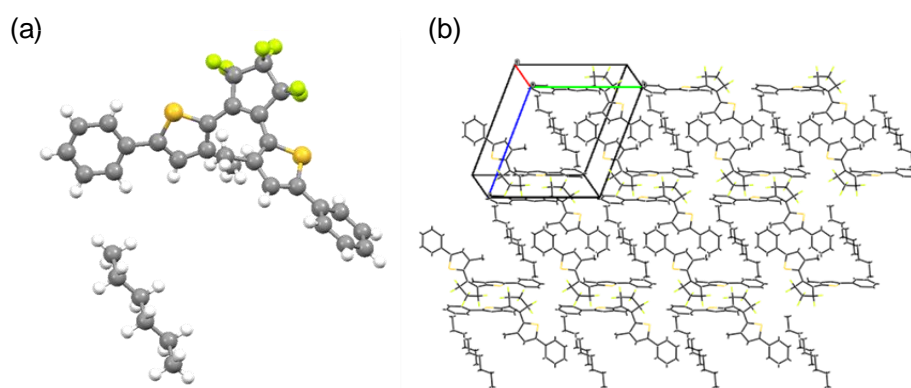


**Fig. 3.** Crystal structure of  $\beta$ -crystal (a) in the asymmetric unit and (b) molecular packing viewed from  $(100)$ . Although there is a half of hexane molecule in the asymmetric unit, whole hexane molecule was illustrated for clarity.

**Table 1.** X-ray crystallographic data for  $\alpha$ - and  $\beta$ -crystals.

	$\alpha$ -crystal	$\beta$ -crystal
Formula	C <sub>27</sub> H <sub>18</sub> F <sub>6</sub> S <sub>2</sub>	C <sub>27</sub> H <sub>18</sub> F <sub>6</sub> S <sub>2</sub> , C <sub>3</sub> H <sub>7</sub>
Formula weight	520.53	563.62
$T/K$	200(2)	200(2)
Crystal system	monoclinic	triclinic
Space group	$P2_1/c$	$P\bar{1}$
$a/\text{\AA}$	17.8941(46)	8.7527(17)
$b/\text{\AA}$	16.9519(5)	12.902(3)
$c/\text{\AA}$	15.9772(5)	13.709(3)
$\alpha/^\circ$	90	110.982(2)
$\beta/^\circ$	102.933(2)	101.756(2)
$\gamma/^\circ$	90	101.938(1)
Volume/ $\text{\AA}^3$	4723.6(3)	1347.24(5)
$Z$	8	2
Density/g cm <sup>-3</sup>	1.464	1.389
Goodness-of-fit on $F^2$	1.166	1.055
$R1 [I > 2\sigma(I)]$	0.0582	0.0528
$wR2$ (all data)	0.1490	0.1425
CCDC No.	1509478	1509479

Next, optical properties of  $\alpha$ - and  $\beta$ -crystals were examined. Fig. 4 shows the diffuse reflection and fluorescence spectra of powder  $\alpha$ - and  $\beta$ -crystals. The optical properties are summarized in Table 2. In the diffuse reflection spectra, both crystals had a strong band around 400 nm and a broad and structureless band in the 450-600 nm region. The absorption edge wavelength of  $\alpha$ -crystal was slightly longer than that of  $\beta$ -crystal. On the other hand, the absorption maximum wavelength and the absorption edge wavelength of **1** in *n*-hexane were observed at 370 and 450 nm, respectively [21]. The difference in the absorption edge wavelength is due to the intermolecular interaction in the crystalline phase. The diarylethene molecules in  $\alpha$ -crystal are packed more closely than that in  $\beta$ -crystal. Although diarylethene **1** undergoes photochromic reactions in *n*-hexane [21], it does not exhibit photochromism in the crystalline state. Moreover, both crystals exhibited strong fluorescence. The fluorescence maximum wavelength ( $\lambda_{\text{flu}}$ ) of  $\beta$ -crystal was observed at 570 nm. On the other hand,  $\lambda_{\text{flu}}$  of  $\alpha$ -crystal was observed at 601 nm, which was shifted toward longer wavelength by 31 nm as compared with those of  $\beta$ -crystal. This is consistent with the difference in the absorption edge wavelength between  $\alpha$ - and  $\beta$ -crystals. Furthermore, the fluorescence quantum yields ( $\Phi_f$ ) and fluorescence lifetime ( $\tau$ ) of  $\alpha$ - and  $\beta$ -crystals were determined as shown in Table 2 and Fig. 5. The  $\Phi_f$  values of  $\alpha$ - and  $\beta$ -crystals were 0.52 and 0.50, respectively, which drastically increased in comparison with that in *n*-hexane ( $\Phi_f = 0.017$ ) [21]. This result clearly indicates that diarylethene **1** has the AIEE character. It is a new type of molecules that exhibit AIEE. The reason why diarylethene **1** shows a strong fluorescence in the crystalline phase may be related to the fact that diarylethene **1** cannot undergo photochromic reactions in the crystalline phase. We are now in the process of investigating the effect of aggregation to photochromic reaction by quantum chemical calculations, results of which will be published in near future.

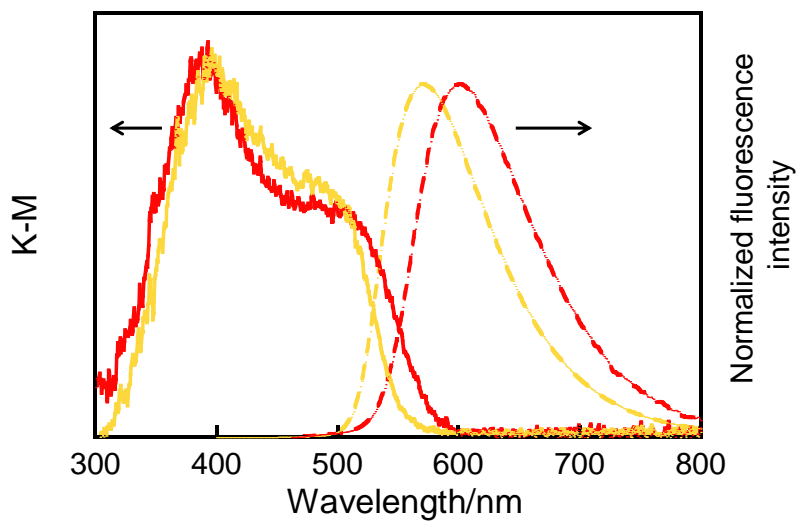


**Fig. 4.** Normalized diffuse reflection spectra (solid line) and fluorescence spectra (dashed line) of powder  $\alpha$ - (orange) and  $\beta$ -crystals (yellow).

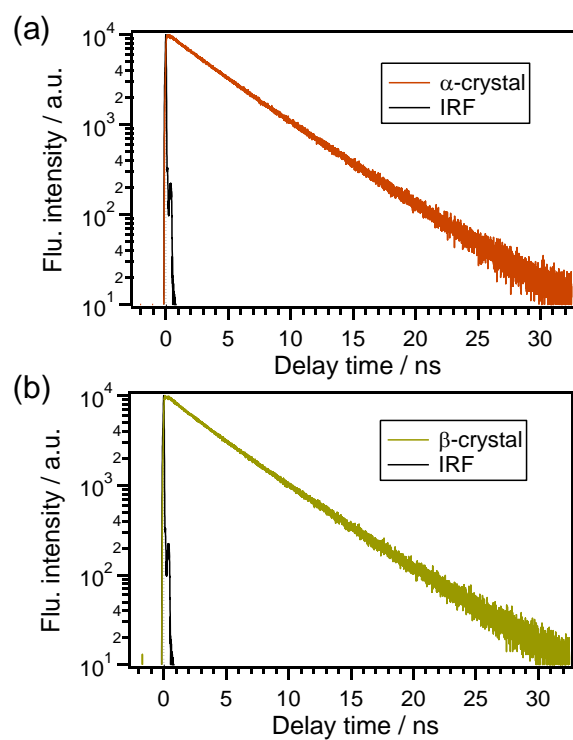


**Fig. 5** Fluorescence decay curves of (a)  $\alpha$ - and (b)  $\beta$ -crystals monitored at 600 nm.

**Table 2.** Absorption and fluorescence spectroscopic data of  $\alpha$ - and  $\beta$ -crystals

	$\lambda_{\text{abs}}/\text{nm}$	$\lambda_{\text{flu}}/\text{nm}$	$\Phi_{\text{f}}^a$	$\tau_1^b/\text{ns}$	$\tau_2^b/\text{ns}$
$\alpha$ -crystal	394, 509	601	0.52	4.6 (89%)	1.9 (11%)
$\beta$ -crystal	398, 505	570	0.50	4.5 (86%)	1.9 (14%)

<sup>a</sup> Excited at 365 nm. <sup>b</sup> Excited at 540 nm and observed at 600 nm.

In the course of this study, we found a polymorphic phase transition from  $\beta$ -form to  $\alpha$ -form. Fig. 6a-b and Video S1 show the optical microscopic photographs observed in reflection mode under irradiation with white light. When the powder  $\beta$ -crystals were heated up from 30 °C to 120 °C at a heating rate of 10 °C min<sup>-1</sup>, the color of the powder crystals changed from yellow to orange. The fluorescence color also changed from yellow to orange, as shown in Fig. 6c-d and Video S2. This color change is not due to isomerization. These results suggest that powder  $\beta$ -crystals can undergo a polymorphic phase transition to  $\alpha$ -form. In order to confirm the phase transition from  $\beta$ -form to  $\alpha$ -form, powder X-ray diffraction measurement was performed. Fig. 7 shows X-ray powder diffraction patterns of the powder  $\beta$ -crystals before and after heating, and the calculated patterns of  $\alpha$ - and  $\beta$ -forms obtained from single-crystal X-ray crystallographic analysis. The diffraction profile after heating was consistent with that of  $\alpha$ -form. This result clearly indicates that the phase transition occurs from  $\beta$ -form to  $\alpha$ -form.

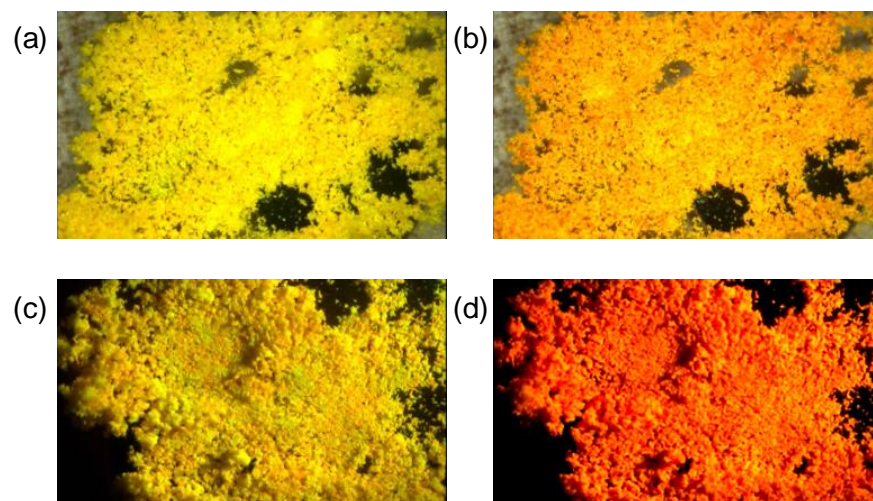


**Fig. 6.** Optical microscopic photographs of powder  $\beta$ -crystals observed in reflection mode under irradiation with white light at (a) 30 and (b) 120 °C, and under excitation with 365 nm light at (c) 30 and (d) 120 °C.

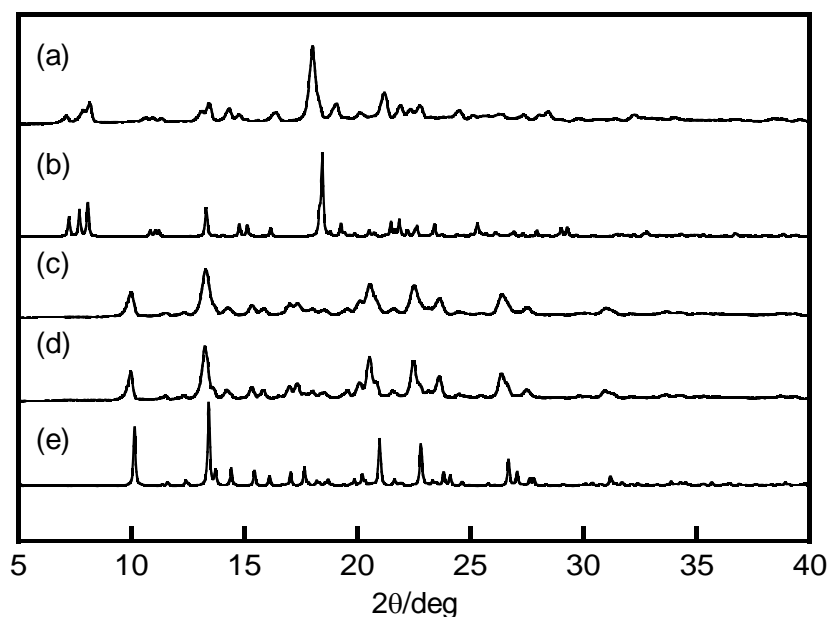


**Fig. 7.** Powder X-ray diffraction patterns: (a) the pattern of powder  $\beta$ -crystals, (b) the calculated pattern of  $\beta$ -crystals, (c) the pattern of after the phase transition of powder  $\beta$ -crystals, (d) the pattern of powder  $\alpha$ -crystals, and (e) the calculated pattern of  $\alpha$ -crystal. The calculated patterns were obtained using parameters determined from single-crystal X-ray crystallographic analysis of  $\alpha$ - and  $\beta$ -forms.

Next, the phase transition from  $\beta$ -form to  $\alpha$ -form was performed in a single crystal. Fig. 8 and Video S3 show the optical microscopic photographs observed at 50 °C under crossed Nicols. The single crystal of  $\beta$ -form emitted yellow (Fig. 8a). After that, the yellow emission became weak (dark state) and the polymorphic phase transition started from the upper right and lower right side, which resulted in the orange emission (Fig. 8b). Finally, the phase transition spread throughout the crystal (Fig. 8c–d). The dark state can be assigned to a low crystallinity state like an amorphous state because the fluorescence quantum yield in the amorphous state ( $\Phi_f = 0.17$ ) is quite smaller than that in the crystalline state ( $\Phi_f \approx 0.5$ ). These results suggest that the polymorphic phase transition from  $\beta$ -form to  $\alpha$ -form includes the collapse of the  $\beta$ -crystalline phase accompanying the exclusion of the hexane molecules and the crystallization of the  $\alpha$ -form. To clarify the exclusion of the hexane molecules, thermogravimetric analysis (TGA) of  $\beta$ -crystal was performed as shown in Fig. 9. When the  $\beta$ -crystal was heated up at a rate of 10 °C min<sup>-1</sup>, the weight of the crystal sample decreased in stepwise. The hexane molecules in the vicinity of the crystal surface were easily excluded around 60 °C. On the other hand, the hexane molecules inside the crystal were excluded at 70–85 °C. The weight loss by the exclusion of the hexane molecules was estimated to be 8%, which is consistent with the amount of the hexane molecules contained in the  $\beta$ -form. Fig. 10 shows the differential scanning calorimetry (DSC) traces of  $\alpha$ - and  $\beta$ -crystals. When the  $\beta$ -crystal was heated up at a rate of 2 °C min<sup>-1</sup>, the crystal showed a small and broad endothermic behavior at 60–80 °C due to the exclusion of the hexane molecules as shown in Fig. S1. After that, a large endothermic and a small exothermic behavior due to the collapse of the  $\beta$ -crystalline phase and crystallization of  $\alpha$ -form and a small endothermic behavior due to the crystal melting were observed at 86–90 °C and around 110 °C, respectively. The  $\alpha$ -crystal exhibited only a large endothermic behavior corresponding to the crystal melting at 120 °C. The melting point of  $\alpha$ -form obtained by the phase transition is lower than that of  $\alpha$ -form prepared by recrystallization. This is ascribed to a low crystallinity or a presence of the amorphous phase. Thus, the results of TGA and DSC measurements are consistent with that observed by fluorescence color change.

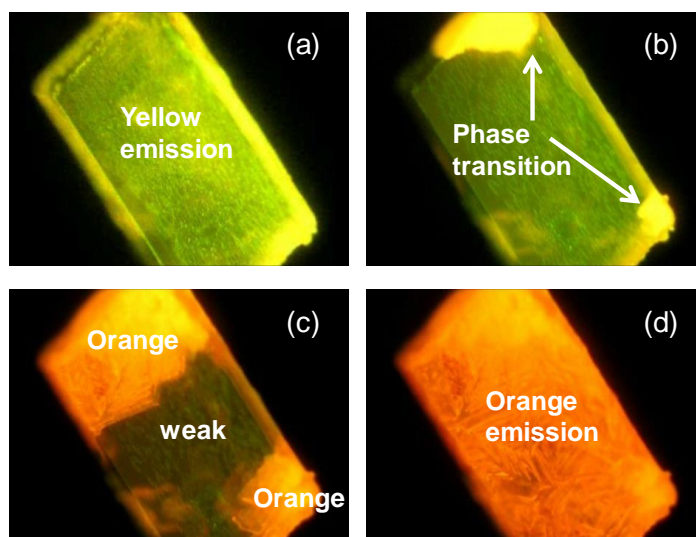


**Fig. 8.** Optical microscopic photographs of  $\beta$ -crystal observed in reflection mode under excitation with 365 nm light at 50 °C , (a) 0, (b) 20, (c) 47, and (d) 80 min later.

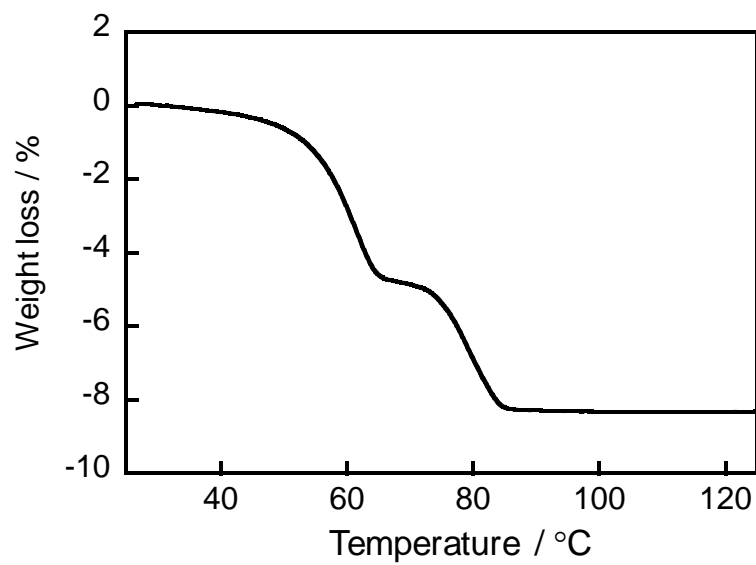


**Fig. 9.** TGA trace of  $\beta$ -crystal at a heating rate of 10 °C min<sup>-1</sup>.



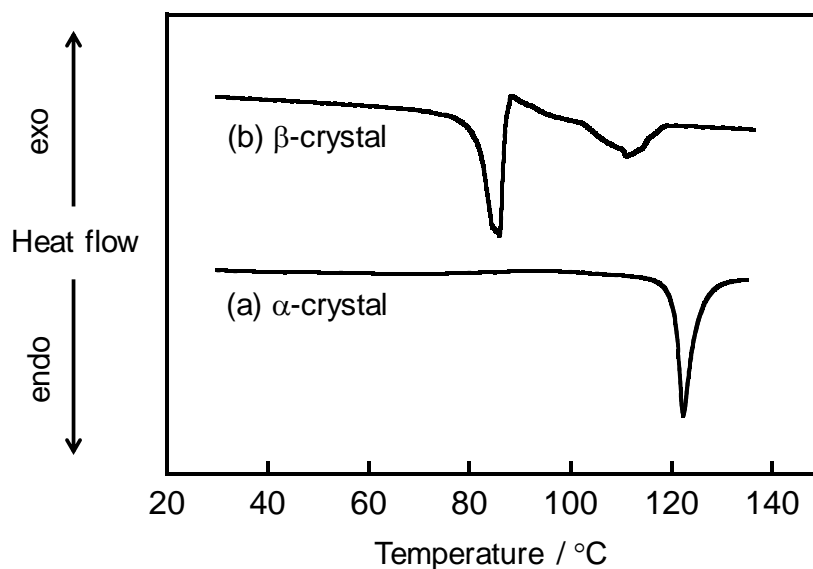


**Fig. 10.** DSC traces of (a)  $\alpha$ - and (b)  $\beta$ -crystals at a heating rate of  $2\text{ }^{\circ}\text{C min}^{-1}$ .

#### 4. Conclusion

We have demonstrated the polymorphism and the phase transition for crystal of diarylethene **1**. Diarylethene **1** has two polymorphic forms,  $\alpha$ - and  $\beta$ -forms. It was revealed that both crystals show strong emission in the crystalline phase as compared with in hexane solution, which means that diarylethene **1** has the AIEE character. We have first observed that the diarylethene exhibits AIEE in the crystalline state. This result provides a new perspective for design of diarylethenes that work as luminescent solid-state materials. Furthermore, the polymorphic phase transition from  $\beta$ -form to  $\alpha$ -form was found and the phase transition process was directly observed by fluorescence color change. In the phase transition process, the fluorescence color changed from yellow to orange via dark state, which means that the phase transition includes the collapse of the  $\beta$ -crystalline phase accompanying the exclusion of the hexane molecules and the crystallization of the  $\alpha$ -form. This mechanism is successfully supported by TGA and DSC measurements. Thus, the polymorphic phase transition process was completely visualized by fluorescence color change.

## Supplementary Data.

Crystallographic data of  $\alpha$ - and  $\beta$ -crystals in CIF format and videos of polymorphic phase transition can be found at <http://dx.doi.org/xx.xxxx/j.dyepig.xxxx.xx.xx>.

## Acknowledgments

This work was partly supported by JSPS KAKENHI Grant Numbers JP26107002, JP2610710, JP26107013 in Scientific Research on Innovative Areas "Photosynergetics", JSPS KAKENHI Grant Number JP16K17896 in Scientific Research for Young Scientists (B) to D.K. and The Murata Science Foundation to D.K. The authors also thank Nippon Zeon Co., Ltd. for providing octafluorocyclopentene.

## References

- [1] Uoyama H, Goushi K, Shizu K, Nomura H, Adachi C. Highly efficient organic light-emitting diodes from delayed fluorescence. *Nature* 2012;492:234–8.
- [2] Zheng JY, Yan Y, Wang X, Zhao YS, Huang J, Yao J. Wire-on-wire growth of fluorescent organic heterojunctions. *J Am Chem Soc* 2012;134:2880–3.
- [3] Duan X, Huang Y, Agarwal R, Lieber CM. Single-nanowire electrically driven lasers. *Nature* 2003;421:241–5.
- [4] Yagai S, Seki T, Aonuma H, Kawaguchi K, Karatsu T, Okura T, Sakon A, Uekusa H, Ito H. Mechanochromic luminescence based on crystal-to-crystal transformation mediated by a transient amorphous state. *Chem Mater* 2016;28:234–41.
- [5] Mutai T, Shono H, Shigemitsu Y, Araki K. Three-color polymorph-dependent luminescence: crystallographic analysis and theoretical study on excited-state

- intramolecular proton transfer (ESIPT) luminescence of cyano-substituted imidazo[1,2-a]pyridine. *CrystEngComm* 2014;16:3890–5.
- [6] Wakamiya A, Mori K, Yamaguchi S. 3-Boryl-2,2'-bithiophene as a versatile core skeleton for full-color highly emissive organic solids. *Angew Chem Int Ed* 2007;46:4273–6.
- [7] Hong Y, Lam JW, Tang BZ. Aggregation-induced emission. *Chem Soc Rev* 2011;40:5361–88.
- [8] Tang, B. Z.; Qin, A. *Aggregation-Induced Emission: Fundamentals*; John Wiley & Sons, 2013.
- [9] Zhang Z, Xu B, Su J, Shen L, Xie Y, Tian H. Color-tunable solid-state emission of 2,2'-biindenyl-based fluorophores. *Angew Chem Int Ed* 2011;50:11654–7.
- [10] Ye X, Liu Y, Lv Y, Liu G, Zheng X, Han Q, Jackson KA, Tao X. In situ microscopic observation of the crystallization process of molecular microparticles by fluorescence switching. *Angew Chem Int Ed* 2015;54:7976–80.
- [11] Ito F, Suzuki Y, Fujimori J, Sagawa T, Hara M, Seki T, Yasukuni R, Lamy de la Chapelle M. Direct visualization of the two-step nucleation model by fluorescence color changes during evaporative crystallization from solution. *Sci Rep* 2016;6:22918.
- [12] Yuan C, Saito S, Camacho C, Irle S, Hisaki I, Yamaguchi S. A  $\pi$ -conjugated system with flexibility and rigidity that shows environment-dependent RGB luminescence. *J Am Chem Soc* 2013;135:8842–5.
- [13] Tachikawa T, Chung H-R, Masuhara A, Kasai H, Oikawa H, Nakanishi H, Fujitsuka M, Majima T. In situ and ex situ observations of the growth dynamics of single perylene nanocrystals in water. *J Am Chem Soc* 2006;128:15944–5.
- [14] Yuan C, Saito S, Camacho C, Kowalczyk T, Irle S, Yamaguchi S. Hybridization of a flexible cyclooctatetraene core and rigid aceneimide wings for multiluminescent flapping  $\pi$  systems. *Chemistry* 2014;20:2193–200.

- [15] Kitagawa D, Yamashita I, Kobatake S. Photoinduced micropatterning by polymorphic crystallization of a photochromic diarylethene in a polymer film. *Chem Commun* 2010;46:3723–5.
- [16] Kitagawa D, Nishi H, Kobatake S. Photoinduced twisting of a photochromic diarylethene crystal. *Angew Chem Int Ed* 2013;52:9320–2.
- [17] Kitagawa D, Kobatake S. Thermodynamic phase transition through crystal-to-crystal process of photochromic 1,2-bis(5-phenyl-2-propyl-3-thienyl)perfluorocyclopentene. *Chem Asian J* 2014;9:289–93.
- [18] Iwaihara C, Kitagawa D, Kobatake S. Polymorphic crystallization and thermodynamic phase transition between the polymorphs of a photochromic diarylethene. *Cryst Growth Des* 2015;15:2017–23.
- [19] Kitagawa D, Kobatake S. Photoreversible current on/off switching by the photoinduced bending of gold-coated diarylethene crystals. *Chem Commun* 2015;51:4421–4.
- [20] Kitagawa D, Okuyama T, Tanaka R, Kobatake S. Photoinduced rapid and explosive fragmentation of diarylethene crystals having urethane bonding. *Chem Mater* 2016;28:4889–92.
- [21] Uchida K, Matsuoka T, Kobatake S, Yamaguchi T, Irie M. Substituent effect on the photochromic reactivity of bis(2-thienyl)perfluorocyclopentenes. *Tetrahedron* 2001;57:4559–65.
- [22] Nagasawa Y, Itoh T, Yasuda M, Ishibashi Y, Ito S, Miyasaka H. Ultrafast charge transfer process of 9,9'-bianthryl in imidazolium ionic liquids. *J Phys Chem B* 2008;112:15758–65.